

Characterization of the climatological variability of mean areal rainfall through fractional coverage

Dong-Jun Seo

Hydrologic Research Laboratory, National Weather Service, Silver Spring, Maryland

James A. Smith

Department of Civil Engineering and Operations Research, Princeton University, Princeton, New Jersey

Abstract. The role of fractional coverage in climatological variability of mean areal rainfall is investigated. Under second-order homogeneity assumptions, climatological variability of mean areal rainfall, as measured by its coefficient of variation, is shown to be a function of mean fractional coverage, conditional coefficient of variation of point rainfall, and two correlation scales associated with inner variability and intermittency of point rainfall. To verify the analytical results, empirical analyses are performed using hourly rainfall data from nine Weather Surveillance Radar—1988 Doppler (WSR-88D) radars in the southern plains, United States. The results indicate that given the local rainfall climatology there exists a catchment scale at which the climatological variability of mean areal rainfall is at its maximum. Existence of such a scale has been hypothesized and demonstrated via an analytical treatment of an idealized situation by *Eagleson and Wang* [1985], but only in climatological variability of fractional coverage (i.e., variability due only to intermittency). Sensitivity analyses for the correlation-scale parameters indicate that intermittency plays as important a role as inner variability in shaping the catchment scale-climatological variability relationship of mean areal rainfall. Decomposition of total variability indicates that over the range of catchment scales that fall within a single WSR-88D radar umbrella (effective radius of 230 km) the integrated contribution from intermittency is almost as large as that from inner variability.

1. Introduction

In large-scale hydrological models and general circulation models the spatial scale of catchments or grid boxes that make up the model domain is relatively large compared to the scale of storm elements. Consequently, rainfall typically occurs only over a fraction of a catchment or a grid box at any time. To assess variabilities or uncertainties associated with model input and output such as mean areal rainfall and areal surface runoff, it is therefore necessary to take into account not only the spatial variability of rainfall within rain area (named “inner variability” in the work by *Barancourt et al.* [1992]) but also the spatial intermittency (i.e., fractional coverage) of rainfall [see *Entekhabi and Eagleson*, 1989].

In this paper, we investigate the role of fractional coverage in climatological variability of mean areal rainfall. Coefficient of variation (CV) is used as the measure of variability. To assess the climatological variability of mean areal rainfall, we first seek expressions for its climatological mean and variance in which both inner variability and intermittency are accounted for. This step constitutes a generalization of the conventional variance-reduction relationship between point and areal rainfall, which implicitly assumes full rainfall coverage at all times [see, e.g., *Rodriguez-Iturbe and Mejia*, 1974]. Then, to verify the expressions derived, empirical analyses are performed using hourly rainfall data from nine WSR-88D (Weather Surveillance Radar—1988 Doppler) radars in the southern plains,

United States. In the work by *Seo and Smith* [1996], related analyses are carried out to assess climatological variability of surface run off under fractional coverage and soil heterogeneity considerations.

The organization of this paper is as follows. In section 2 we derive expressions for climatological mean and variance of mean areal rainfall. In section 3 we describe the radar rainfall data used in this work. In section 4 we describe the empirical analyses and verification of the expressions derived. In section 5, conclusions are presented.

2. Moments of Mean Areal Rainfall

Let us define $R(u, t)$ as the rain rate at location u at time t . Then, mean areal rainfall over the catchment of area $\|A\|$ at time t , $M(A, t)$, is given by

$$M(A, t) = \|A\|^{-1} \int_A R(u, t) du \quad (1)$$

To consider only the fractional coverage situations, we assume that $R(u, t) > 0$ somewhere in A . Throughout this paper, this conditioning is not explicitly denoted in expectation and probability expressions for the sake of brevity. Unless mentioned otherwise, expectations and probabilities are to be understood as conditional on occurrence of rainfall somewhere in A .

Expectation or climatological mean of $M(A, t)$ is then given by

$$E[M(A, t)] \equiv m_M(A, t) \quad (2a)$$

Copyright 1996 by the American Geophysical Union.

Paper number 96WR00486.
0043-1397/96/96WR-00486\$09.00

$$E[M(A, t)] = \|A\|^{-1} \int_A E[R(u, t)|R(u, t) > 0] \cdot Pr[R(u, t) > 0] du \tag{2b}$$

where the expectations are taken with respect to time. To express $Pr[R(u, t) > 0]$ in terms of fractional coverage, we define an indicator random variable, $I[R(u, t); 0]$, as follows:

$$i[R(u, t); x] = 1 \quad R(u, t) > x \tag{3}$$

$$i[R(u, t); x] = 0 \quad \text{otherwise}$$

where x is some threshold value and $i[R(u, t); x]$ denotes the experimental value of $I[R(u, t); x]$. From the definition of (3) we have

$$Pr[R(u, t) > 0] = E\{I[R(u, t); 0]\} \tag{4}$$

Fractional coverage of rainfall over catchment A at time t , $Z(A, t)$, can be represented by

$$Z(A, t) = \|A\|^{-1} \int_A I[R(u, t); 0] du \tag{5}$$

Assuming that $I[R(u, t); 0]$ is homogeneous in A (i.e., occurrence of rainfall is equally likely everywhere within A), we may write

$$E[Z(A, t)] \equiv m_Z(A, t) \tag{6a}$$

$$E[Z(A, t)] = E\{I[R(u, t); 0]\} \tag{6b}$$

where $m_Z(A, t)$ is the climatological mean of fractional coverage. Assuming that $R(u, t)$ is homogeneous within A , we may write

$$E[R(u, t)|R(u, t) > 0] = m_R(t) \tag{7}$$

where $m_R(t)$ is the climatological conditional mean of point rainfall. Hence, for the climatological mean of $M(A, t)$ we have

$$m_M(A, t) = m_R(t)m_Z(A, t) \tag{8}$$

The expression for the climatological variance of mean areal rainfall may be obtained as follows. Let us first consider

$$M^2(A, t) = \|A\|^{-2} \int_A \int_A R(u, t)R(v, t) du dv \tag{9}$$

Expectation of $M^2(A, t)$ is given by

$$E[M^2(A, t)] = \|A\|^{-2} \cdot \int_A \int_A E[R(u, t)R(v, t)|R(u, t) > 0, R(v, t) > 0] \cdot Pr[R(u, t) > 0, R(v, t) > 0] du dv \tag{10}$$

Assuming that both $R(u, t)$ and $I(R(u, t); 0)$ are second-order homogeneous within A , we may parameterize the terms in the integrand in (10) as follows:

$$E[R(u, t)R(v, t)|R(u, t) > 0, R(v, t) > 0] = \sigma_R^2(t)\rho_R[|u - v|; L_{SR}(t)] + m_R^2(t) \tag{11}$$

$$Pr[R(u, t) > 0, R(v, t) > 0] \equiv E\{I[R(u, t); 0]I[R(v, t); 0]\} \tag{12a}$$

$$Pr[R(u, t) > 0, R(v, t) > 0] = m_Z(A, t) \cdot \{1 - m_Z(A, t)\}\rho_I[|u - v|; L_{SI}(t)] + m_Z^2(A, t) \tag{12b}$$

In (11) and (12b), $\sigma_R^2(t)$ is the conditional variance of point rainfall at time t , $\rho_R[|u - v|; L_{SR}(t)]$ is the conditional correlation function of point rainfall, where $|u - v|$ is the Euclidian distance between the two points u and v , and $L_{SR}(t)$ is the conditional correlation-scale parameter at time t , $\rho_I[|u - v|; L_{SI}(t)]$ is the climatological indicator correlation function where $L_{SI}(t)$ is the indicator correlation-scale parameter at time t .

Equations (11) and (12b) follow directly from the definitions of conditional and indicator covariances, respectively, under the second-order homogeneity conditions. In arriving at (12b) we also have used the identities, $\text{Var}\{I[R(u, t); 0]\} \equiv E\{I[R(u, t); 0]\} \{1 - E\{I[R(u, t); 0]\}\} = m_Z(A, t) \{1 - m_Z(A, t)\}$. Similar parameterizations have been used in previous studies of spatial variability of radar rainfall [Seo and Smith, 1991; Seo, 1995]. Hence, for the climatological variance of mean areal rainfall, $\sigma_M^2(A, t)$, we have

$$\sigma_M^2(A, t) = \sigma_R^2(t)m_Z(A, t)\{1 - m_Z(A, t)\}\|A\|^{-2} \cdot \int_A \int_A \rho_R[|u - v|; L_{SR}(t)]\rho_I[|u - v|; L_{SI}(t)] du dv + \sigma_R^2(t)m_Z^2(A, t)\|A\|^{-2} \cdot \int_A \int_A \rho_R[|u - v|; L_{SR}(t)] du dv + m_R^2(t)m_Z(A, t)\{1 - m_Z(A, t)\}\|A\|^{-2} \cdot \int_A \int_A \rho_I[|u - v|; L_{SI}(t)] du dv \tag{13}$$

Note that if $m_Z(A, t) = 1$ (i.e., full rainfall coverage), (13) reduces to the conventional variance-reduction relationship between point and areal rainfall [see, e.g., Rodriguez-Iurbe and Mejia, 1974]. Note also that because of the cross terms between (11) and (12b), $\sigma_M^2(A, t)$ depends also on $m_R(t)$. Owing to this dependence on letting $R(u, t) = 1$ for all $u, u \in A_c$, where A_c denotes the rain area within A , we have the following identity from (13) between $\sigma_Z^2(A, t)$ and $m_Z(A, t)$:

$$\sigma_M^2(A, t) \equiv \sigma_Z^2(A, t) \tag{14a}$$

$$\sigma_M^2(A, t) = m_Z(A, t)\{1 - m_Z(A, t)\}\|A\|^{-2} \cdot \int_A \int_A \rho_I[|u - v|; L_{SI}(t)] du dv \tag{14b}$$

From (8) and (13) we have for the climatological CV of mean areal rainfall over A at time t , $CV_M(A, t)$:

$$CV_M(A, t) = \left\{ CV_R^2(t)[1/m_Z(A, t) - 1]\|A\|^{-2} \right.$$

$$\begin{aligned}
 & \cdot \int_A \int_A \rho_R(|u - v|; L_{SR}(t)) \rho_I(|u - v|; L_{SI}(t)) du dv \\
 & + CV_R^2(t) \|A\|^{-2} \int_A \int_A \rho_R(|u - v|; L_{SR}(t)) du dv \\
 & + [1/m_Z(A, t) - 1] \|A\|^{-2} \\
 & \cdot \left. \int_A \int_A \rho_I(|u - v|; L_{SI}(t)) du dv \right\}^{1/2} \quad (15)
 \end{aligned}$$

where $CV_R(t)$ is the conditional CV of point rainfall at time t . Sensitivities of $CV_M(A, t)$ on $CV_R(t)$, $L_{SR}(t)$, and $L_{SI}(t)$ will be shown later in the paper. Similarly, from (14) we have for the climatological CV of fractional coverage, $CV_Z(A, t)$:

$$\begin{aligned}
 CV_Z(A, t) = & \left\{ [1/m_Z(A, t) - 1] \|A\|^{-2} \int_A \int_A \rho_I[|u \right. \\
 & \left. - v|; L_{SI}(t)] dudv \right\}^{1/2} \quad (16)
 \end{aligned}$$

Sensitivity of $CV_Z(A, t)$ on $L_{SI}(t)$ will also be shown later in the paper. Noting that the last term in the right-hand side of (15) is the same as $CV_Z^2(A, t)$ in (16), we see that the second and the third terms in the right-hand side of (15) represent contributions from inner variability and intermittency, respectively (the first being the cross term). This enables quantitative decomposition of $CV_M^2(A, t)$, as will be shown later in the paper.

3. Description of Data

The data used in this work are hourly rainfall fields from a network of nine WSR-88D radars in the southern plains, United States, a subset of the national Next Generation Weather Radar (NEXRAD) network. The radars are located at or near Denver, Colorado (FTG), Goodland, Kansas (GLD), Amarillo, Texas (AMA), Dodge City, Kansas (DDC), Frederick, Oklahoma (FDR), Wichita, Kansas (ICT), Twin Lakes, Oklahoma (TLX), Tulsa, Oklahoma (INX), and Little Rock, Arkansas (LZK). The data cover the period of late August 1993 through early May 1994. Figure 1 shows the radar umbrellas (effective range of 230 km) on the area map.

The particular type of data used in this work is known as the "hourly digital precipitation array," a derived product from an algorithm called the precipitation processing subsystem [Hudlow, 1988; Klazura and Imy, 1993]. At each radar site the array constitutes a 131×131 mesh, overlaid onto the Hydrologic Rainfall Analysis Project grid system (D. R. Greene and M. Hudlow, unpublished manuscript, 1982). The mesh size, which is a function of latitude, is approximately 4×4 km² over the study area.

As with any other radar rainfall data, the data used in this work possess certain error characteristics of their own. For detailed studies on the quality of NEXRAD precipitation products, the reader is kindly referred to Smith and Krajewski [1994], Seo et al. [1995], and Smith et al. [1996]. We only note here that the data went through a series of quality control steps including extensive visual inspections and are considered of good quality for the type of analyses performed in this work. The minimum hourly rainfall was 0.1 mm for the data.

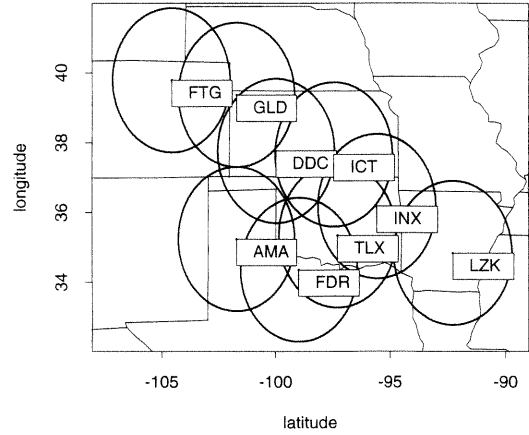


Figure 1. Area map with radar umbrellas.

4. Empirical Analyses and Verification

Because rainfall processes are in general nonstationary, the expressions for the climatological mean and variance of mean areal rainfall (equations (8) and (13)) are written as functions of time (or, more practically, time elapsed since the initiation of rain). To estimate the statistics and the parameters in (8) and (13) as time-varying variables, however, a very large amount of data would be required, as well as their stratification with respect to seasonality, type of storm, and stage of storm development, etc. To circumvent these difficulties, stationarity was assumed in this work. The statistics and the parameters were then estimated by pooling samples from radar rainfall fields taken every 5 hours. Although it substantially reduced the amount of data available for the analyses, the sampling interval of 5 hours was necessary to ensure temporal independence between successive fields (for details, see Seo and Smith [1996]), thereby minimizing overrepresentation by widespread rainfall fields. During the period covered by the data there were approximately 40 storms (meso- β scale or larger) observed within the composite area covered by the nine radars. The number of hourly rainfall fields used in the analyses varied from 94 to 310, depending on the site.

4.1. Estimation of Correlation-Scale Parameters

The conditional correlation-scale parameter $L_{SR}(t)$ was estimated from long-term conditional correlograms of point rainfall. Figure 2 shows an example of the directional correlograms at FDR. At some sites, anisotropy was clearly evident. At other sites, nonhomogeneity or periodicity was suspected. Table 1 summarizes $L_{SR}(t)$ at all sites, as estimated from fitting a two-parameter (nugget effect and range) isotropic exponential model of the following form:

$$\begin{aligned}
 \rho_R[|u - v|; L_{SR}(t)] = & [1 - \mu(t)] \exp[-|u - v|/L_{SR}(t)] \\
 & |u - v| > 0 \quad (17) \\
 \rho_R[|u - v|; L_{SR}(t)] = & 1 \quad |u - v| = 0
 \end{aligned}$$

where $\mu(t)$ is the nugget effect. In the table, for those sites where nonhomogeneity and/or strong anisotropy is present, the estimated correlation scale is likely to be an overestimate.

The indicator correlation-scale parameter $L_{SI}(t)$ was estimated from long-term bivariate joint probabilities or, equiva-

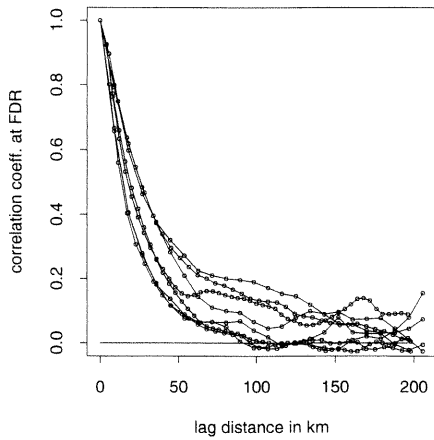


Figure 2. Conditional correlograms of point rainfall at FDR along eight directions (0° , 26.6° , 45° , 63.4° , 90° , 116.6° , 135° , and 153.4°).

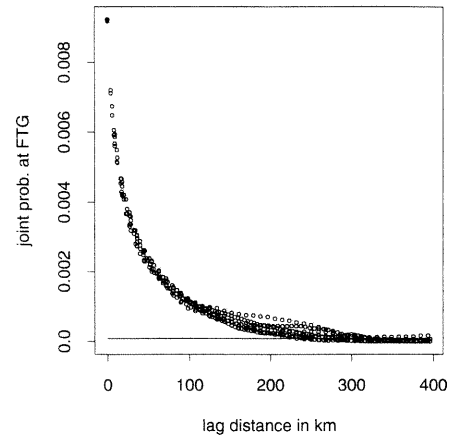


Figure 3. Experimental noncentered indicator covariance functions at FTG along eight directions (0° , 26.6° , 45° , 63.4° , 90° , 116.6° , 135° , and 153.4°).

lently, noncentered indicator covariances. Figures 3 and 4 show examples of the experimental directional joint probabilities at FTG and LZK, respectively. Table 1 summarizes $L_{SI}(t)$ at all sites as estimated by fitting a model analogous to (17). The estimates of $L_{SI}(t)$ are a reflection of the life history of storms in the southern plains: In the west, where storms are born, $L_{SI}(t)$ tends to be smaller (cellular-structured rainfall fields), and as they move eastward maturing and dissipating, $L_{SI}(t)$ tends to be larger (more widespread rainfall fields). Table 1 also summarizes $m_R(t)$ and $CV_R(t)$ at all sites.

4.2. Observed Mean Fractional Coverage

Figure 5 shows observed $m_Z(A, t)$ as a function of A at all sites. Because the spatial resolution of the radar used in this work is $4 \times 4 \text{ km}^2$, we have, by definition (see equation (1)), $M_Z(A, t) = 1$ at that spatial scale. For larger values of A , $M_Z(A, t)$ is a monotonically decreasing function because on the average the larger the catchment, the smaller the fractional coverage of rainfall. For yet larger values of A we may expect $M_Z(A, t)$ to asymptotically reach a limit because within a very large area there may always exist at least a single storm at any given time. Figure 5 shows the shift in climatology of fractional coverage of rainfall in the southern plains: $m_Z(A, t)$ increases as one moves from the northwest to the southeast. It indicates that on the average the spatial extent of rainfall systems is smaller in the northwest and larger in the southeast (see also $L_{SI}(t)$ in Table 1).

4.3. Observed and Predicted Variabilities of Fractional Coverage

CV of fractional coverage represents climatological variability of mean areal rainfall due strictly to intermittency. Figures 6 and 7 show the observed $m_Z(A, t)$ (solid line), $\sigma_Z^2(A, t)$ (marked by “v”), and $CV_Z(A, t)$ (marked by “c”) as functions of A at FTG and INX, respectively. Also shown in Figures 6 and 7 are the predicted (marked by “+”) $\sigma_Z^2(A, t)$ and $CV_Z(A, t)$ as obtained from (14b) and (16), respectively. Figures 6 and 7 are equivalent to Figure 5 of *Eagleson and Wang* [1985] with A_S , or storm size, in the reference held constant. Figure 8 shows the series of grid boxes used to represent square catchment areas within the coverage of a single radar umbrella. Innermost boxes are centered away from the radar site because, at closer ranges the sampling strategy for rain estimation is different from that at the outer range, producing disparate error characteristics [*Smith and Krajewski*, 1994, *Seo et al.*, 1995; *Smith et al.*, 1996].

In Figures 6 and 7 the observed relationships between $\sigma_Z^2(A, t)$ and \sqrt{A} are in good agreement with what is expected from (14b): With $\sigma_Z^2(A, t)$ being a quadratic function of $m_Z(A, t)$ with roots at 0 and 1, while $\|A\|^{-2} \int_A \int_A \rho_i[|u - v|; L_{SI}(t)] dudv$ is a monotonic, slowly decreasing function of A from 1 to 0 on $(0, \infty]$, $\sigma_Z^2(A, t)$ has the maximum near $m_Z(A, t) \approx \frac{1}{2}$ and approaches zero as $A \rightarrow 0$ or $A \rightarrow \infty$. The predicted relationships between $\sigma_Z^2(A, t)$ and \sqrt{A} are in reasonably good agreement with the observed ones; underrepresentation of

Table 1. Radar Rainfall Statistics at Nine WSR-88D Sites

	Site								
	FTG	GLD	AMA	DDC	FDR	ICT	TLX	INX	LZK
$L_{SI}(t)$, km	33.7	52.5	73.0	57.0	68.6	62.6	81.4	82.5	80.1
$L_{SR}(t)$, km	33.7 ^a	27.3 ^b	41.9 ^a	31.5	28.8	39.6 ^a	29.3	30.3	46.7 ^c
$L_{SI}(t)/L_{SR}(t)$	1.0	1.9	1.7	1.8	2.4	1.6	2.8	2.7	1.7
$m_R(t)$, mm	1.10	1.37	2.06	1.71	1.86	2.56	1.78	2.39	2.45
$CV_R(t)$	2.23	2.49	2.01	1.97	2.00	1.99	1.73	1.76	1.64

^aNonhomogeneity suspected.
^bPeriodicity present.
^cStrong anisotropy present.

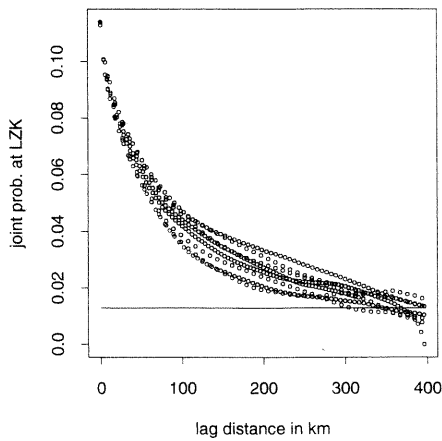


Figure 4. Same as Figure 3, but at LZK.

very small or very large fractional coverage situations in the limited data sets is likely to be responsible for the tendency to underpredict $\sigma_z^2(A, t)$ seen in Figures 6 and 7. The predicted relationships between $CV_z(A, t)$ and \sqrt{A} are also in reasonably good agreement with the observed ones. Examination of the scale-variability relationships of mean areal rainfall at all sites indicates that observed $CV_z(A, t)$ peaks near $\sqrt{A} \approx 120\text{--}200$ km. The catchment scale associated with the maximum CV will be denoted as A_p . Unfortunately, the maximum window size within a single radar umbrella is not large enough to ascertain the relationship at larger values of A . It is, however, possible to conjecture from the following argument that $CV_z(A, t)$ is a slowly and monotonically decreasing function of A , as $A \rightarrow \infty$. For large A we may write $CV_z(A, t) \approx |A|^{-2} \int_A \int_A \rho_1[|u - v|; L_{SI}(t)] dudv / m_z(A, t)$ (see equation (16)). If A is sufficiently large, multiple storms may coexist undergoing life cycles independently of one another, in which case a constant $m_z(A, t)$ may be assumed. Hence, for a very large A we have $CV_z(A, t) \propto |A|^{-2} \int_A \int_A \rho_1[|u - v|; L_{SI}(t)] du dv$, which is a monotonically decreasing function of A .

Figure 9 shows sensitivity of $CV_z(A, t)$ on $L_{SI}(t)$, assuming

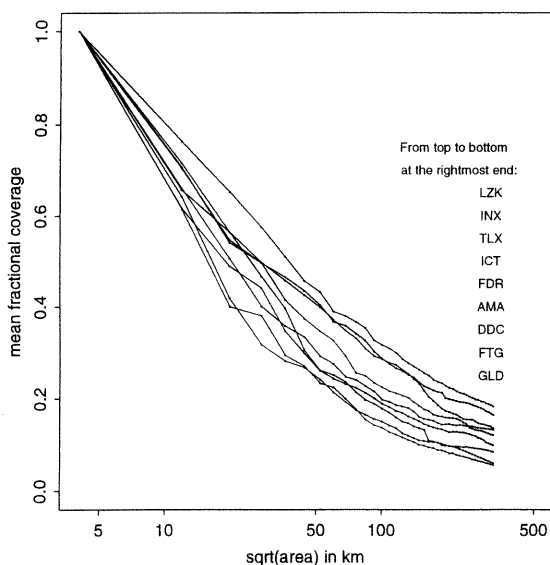


Figure 5. Observed $m_z(A, t)$ at all sites.

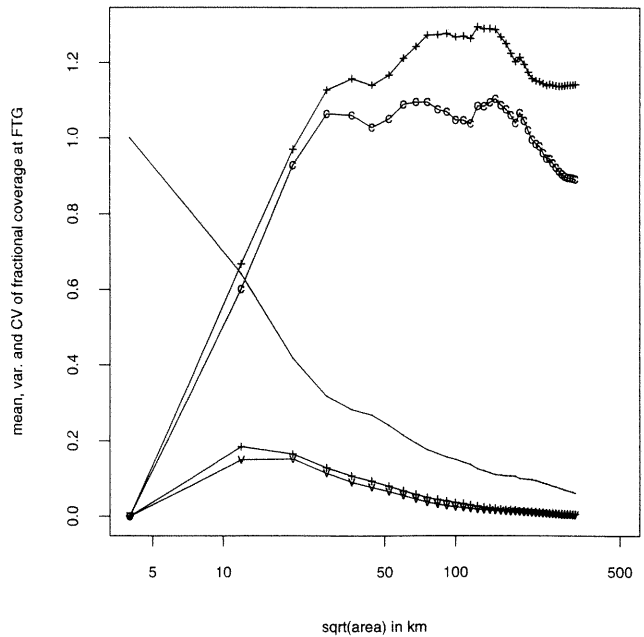


Figure 6. Observed $\sigma_z^2(A, t)$ (marked by “v” in the bottom pair of curves), predicted $\sigma_z^2(A, t)$ (marked by plus sign in the bottom pair of curves), observed $CV_z(A, t)$ (marked by “c” in the top pair of curves), and predicted $CV_z(A, t)$ (marked by plus sign in the top pair of curves) at FTG.

a fixed relationship between $m_z(A, t)$ and A . In producing Figure 9 we have used for $\rho_1[|u - v|; L_{SI}(t)]$ in (16) the Gaussian model with no nugget effect [Journel and Huijbregts, 1978, p. 165] in place of the exponential model with nugget effect (see equation (17)). Although it is a less accurate representation of the observed correlation structure, particularly near the origin, the assumption obviates numerical integration of the quadruple integral (see appendix). The unconnected

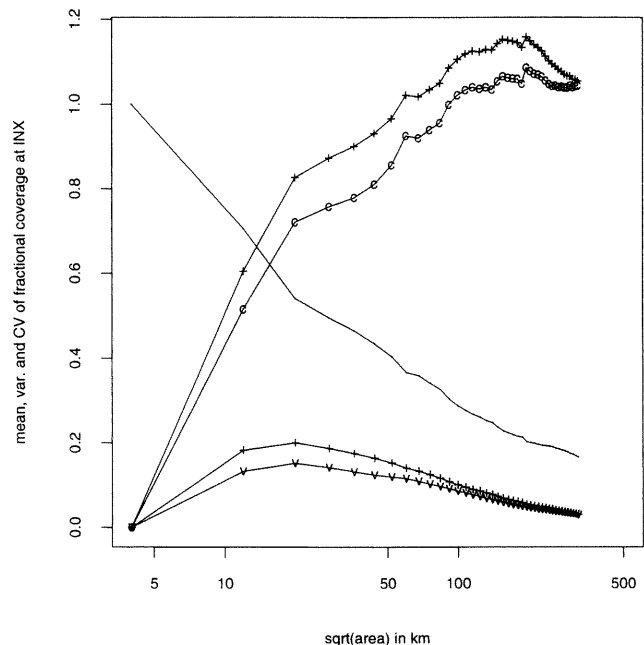


Figure 7. Same as Figure 6, but at INX.

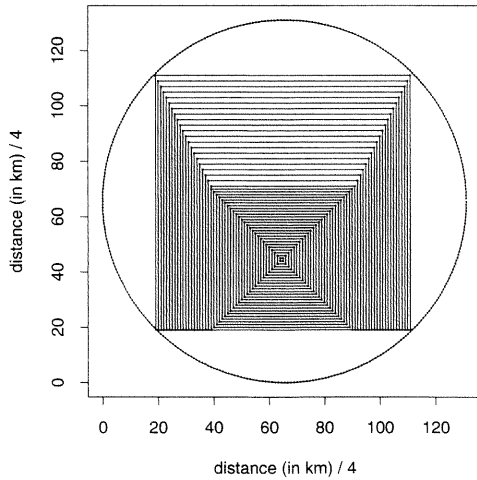


Figure 8. Sampling windows within a WSR-88D radar umbrella.

markers represent the reference relationship based on observed parameter values and statistics at ICT. The increment in $L_{SI}(t)$ is 10 km. Note that an increase in $L_{SI}(t)$ (i.e., increase in storm sizes) not only increases A_p but also the magnitude of peak variability due to intermittency, $CV_Z(A_p, t)$.

4.4. Observed and Predicted Variabilities of Mean Areal Rainfall

CV of mean areal rainfall represents climatological variability of mean areal rainfall due to both intermittency and inner variability. Figures 10 and 11 show $CV_M(A, t)$ as a function of A at FDR and LZK, respectively. For comparison purposes, $CV_Z(A, t)$ is also shown. In Figures 10 and 11 there are two pairs of curves, the upper and lower pairs representing $CV_M(A, t)$ and $CV_Z(A, t)$, respectively. In each pair the observed and the predicted values are marked by open circles and plus signs, respectively. An ideal situation in obtaining predicted values of $CV_M(A, t)$ from (15) would be to have a sufficiently large amount of data so that the observed values of $CV_R(t)$ are indeed catchment scale-invariant. Unfortunately, such was not the case in this work and, hence, to correct for the

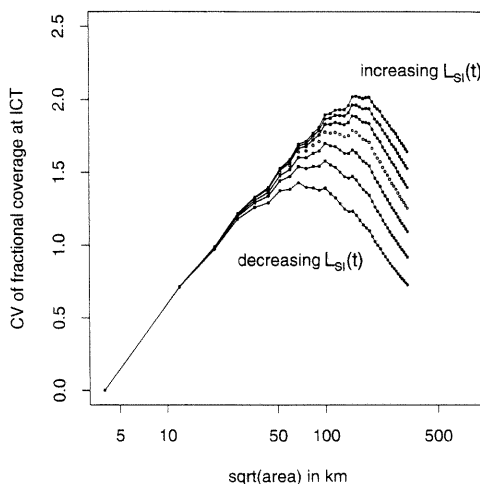


Figure 9. Sensitivity of $CV_Z(A, t)$ on $L_{SI}(t)$ (unconnected markers are based on the observed parameter values).

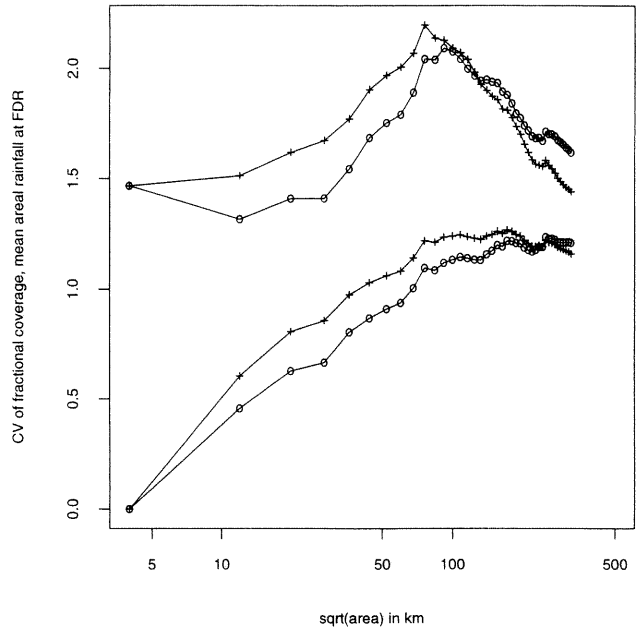


Figure 10. Observed $CV_M(A, t)$ (marked by open circles in the top pair of curves), predicted $CV_M(A, t)$ (marked by plus signs in the top pair of curves), observed $CV_Z(A, t)$ (marked by open circles in the bottom pair of curves) and $CV_Z(A, t)$ (marked by plus signs in the bottom pair of curves) at FDR.

scale-dependency effect of $CV_R(t)$, we used sample statistics of $CV_R(t)$ estimated as a function of A .

At five out of nine sites, clear unimodal peaks exist in observed $CV_M(A, t)$ (see Figures 10 and 11). At other sites, peaks are not necessarily unimodal or no clear peaks exist. In the cases where clear unimodal peaks exist, A_p (i.e., the catchment scale at which the peak CV occurs) in observed $CV_M(A, t)$ tends to be smaller than that in observed $CV_Z(A, t)$ ($\sqrt{A_p} \approx 30\text{--}80$ km for mean areal rainfall versus $\sqrt{A_p} \approx 110$ km or

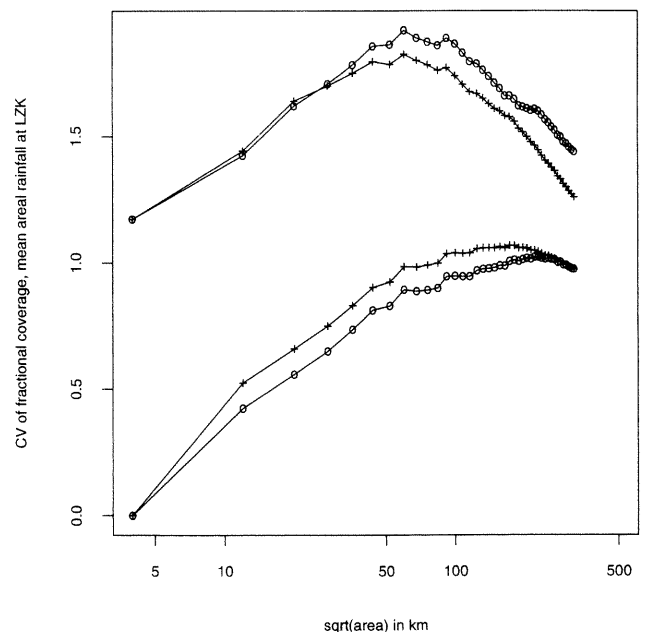


Figure 11. Same as Figure 10, but at LZK.

larger for fractional coverage). It suggests that adding inner variability to intermittency reduces A_p because inner variability is generally characterized by a smaller correlation scale (i.e., $L_{SR}(t) < L_{SI}(t)$, see Table 1).

In general, the observed scale-variability relationships of mean areal rainfall are in reasonably good agreement with those predicted by (15). For those sites where nonhomogeneity or periodicity is suspected (see Table 1), predictions tend to deviate. There are a number of factors contributing to the discrepancies between the observed and the predicted relationships: (1) conditional and/or indicator second-order statistics of point rainfall may not be homogeneous, (2) data size is not large enough to produce "climatological" variabilities, (3) correlation structures are not accurately modeled at all lag distances, and (4) the scale parameters may be time-dependent (especially on seasonality).

Figures 12 and 13 show decomposition of $CV_M^2(A, t)$ into contributions from intermittency and inner variability (see equation (15)) at GLD and TLX, respectively. As expected, climatological variability of mean areal rainfall is dominated by inner variability over smaller A and by intermittency over larger A . Inner variability and intermittency are at balance near $\sqrt{A} \approx 40\text{--}60$ km. The coverage of a single radar is seen to capture, at least in the southern plains, most of the range of catchment scales over which transition from inner variability dominance to intermittency dominance takes place. Table 1 shows the ratio of $L_{SI}(t)$ to $L_{SR}(t)$ at all sites, in which TLX has a significantly higher ratio (i.e., strong intermittency) than GLD (i.e., weak intermittency). This is also reflected in Figures 12 and 13 where the area designated as "intermittency" (this is the percent contribution of intermittency integrated over all catchment scales that fall within the radar umbrella) is substantially larger for TLX.

Figures 14, 15, and 16 show sensitivities of $CV_M(A, t)$ on $CV_R(t)$, $L_{SI}(t)$ and $L_{SR}(t)$, respectively. As in producing Figure 9, Gaussian models were assumed for both $\rho_R[|u - v|; L_{SR}(t)]$ and $\rho_I[|u - v|; L_{SI}(t)]$ to avoid numerical integra-

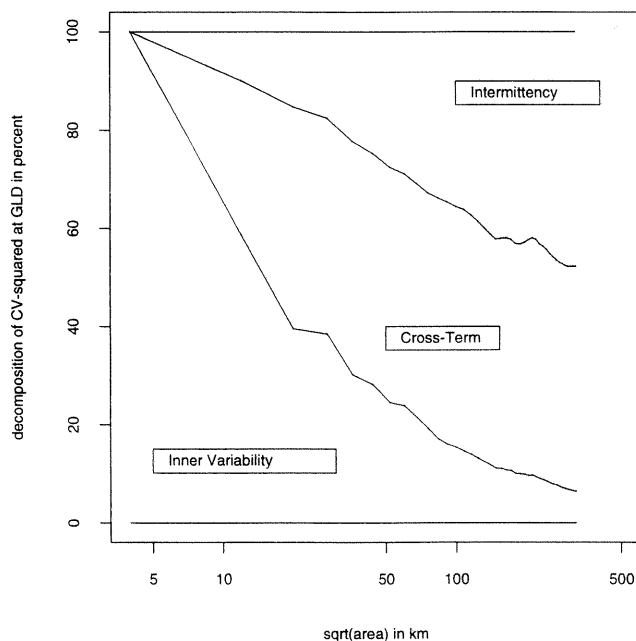


Figure 12. Decomposition of $CV_M^2(A, t)$ at GLD.

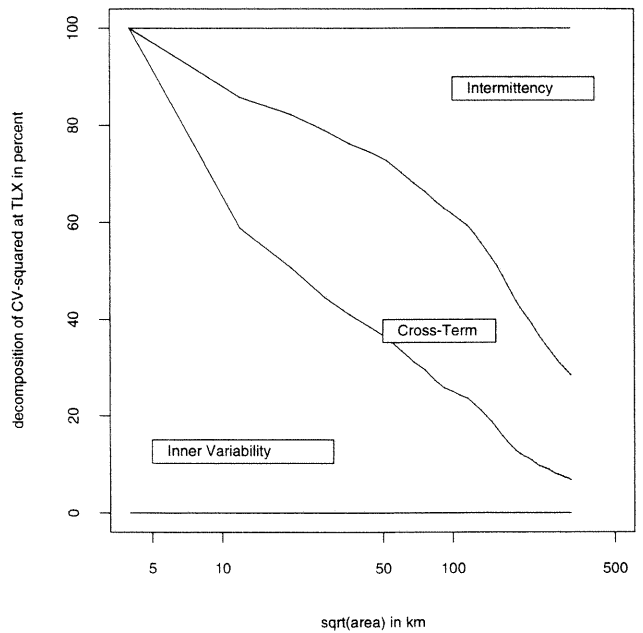


Figure 13. Same as Figure 12, but at TLX.

tions. The unconnected markers represent reference relationships based on observed parameter values and statistics at LZK. The increments are 10 km for $L_{SR}(t)$ and $L_{SI}(t)$ and 0.5 for $CV_R(t)$. They illustrate that each parameter has a varying and unique effect on the scale-variability relationship of mean areal rainfall.

5. Conclusions

Under the assumption that both conditional (on occurrence of rain) and indicator second-order statistics of point rainfall are homogeneous, climatological variability of mean areal rainfall, as measured by its coefficient of variation, is shown to be a function of mean fractional coverage, conditional coefficient of variation of point rainfall, conditional correlation function of point rainfall, and indicator correlation function of

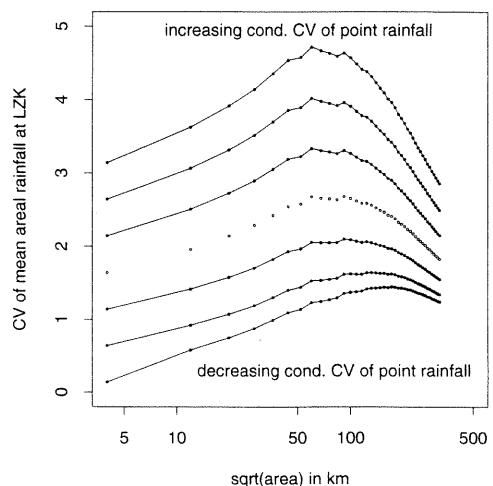


Figure 14. Sensitivity of $CV_M(A, t)$ on $CV_R(t)$ (unconnected markers are based on the observed parameter values).

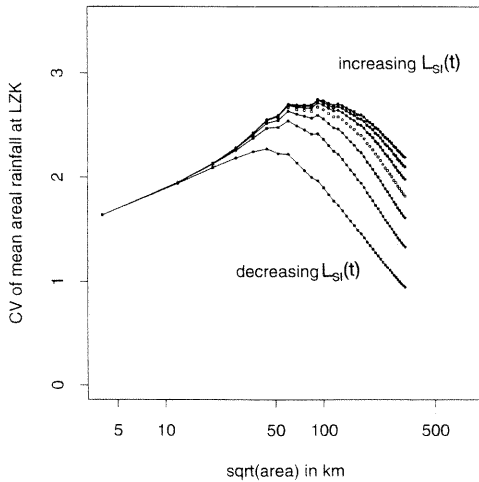


Figure 15. Same as Figure 14, but on $L_{Sl}(t)$.

point rainfall. The expressions for CV of mean areal rainfall and fractional coverage are verified via empirical analyses using hourly rainfall data from nine WSR-88D radars in the southern plains. The analyses indicate that given the local rainfall climatology there exists a unique catchment scale at which the climatological variability of mean areal rainfall is at its maximum. Existence of such a scale in climatological variability of fractional coverage [Eagleson and Wang, 1985], however, is seen to be less prominent, at least over the range of catchment scales examined in this work. Sensitivity analyses on the correlation-scale parameters indicates that intermittency plays as important a role as inner variability in shaping the catchment-scale-climatological variability relationship of mean areal rainfall. Decomposition of total variability indicates that over the range of catchment scales that fall within a single WSR-88D radar umbrella (effective radius of 230 km), the integrated contribution from intermittency is almost as large as that from inner variability.

The scale-variability relationships of mean areal rainfall shown in the work indicate that even with appropriate subgrid-scale parameterizations, decreasing the grid scale in large-scale hydrological or GCM models (say, from 200 to 100 km) is

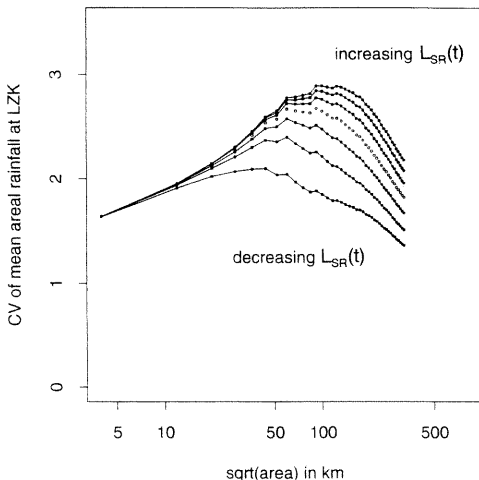


Figure 16. Same as Figure 14, but on $L_{SR}(t)$.

likely to increase the uncertainty in model output because of the increased variability in mean areal rainfall. In other words, in choosing the grid size, there is a trade-off to consider between more uncertain model output with higher spatial resolution and less uncertain model output with lower spatial resolution. This aspect is particularly relevant, for example, to the Global Energy and Water Experiment (GEWEX) Continental-scale International Project (GCIP) modeling strategy, for which parameterization of energy and water cycle processes is to be developed at 100-km scale [World Meteorological Organization and the International Council of Scientific Unions, 1992]. The scale-variability relationships obtained in this work should also be useful in assessing uncertainties associated with mean areal rainfall input to operational rainfall-runoff models such as the National Weather Service River Forecast System [Anderson, 1973]. The analytical results obtained in this work should be useful in converting rainfall at one spatial scale to another under fractional coverage conditions. Likewise, analogous results in time domain should be useful in converting point rainfall at one temporal scale to another under intermittency conditions.

Finally, the empirical analyses performed in this work demonstrate that WSR-88D rainfall data are extremely useful in climatological studies. To obtain climatologically more representative results and to examine the scale-variability relationships over larger catchment areas, systematic archiving, quality control, and mosaicking of WSR-88D rainfall data are essential.

Appendix

Here we evaluate the quadruple integral of the following form:

$$I = \int_A \int_A \rho(|v - u|; L) du dv \tag{A1}$$

where A is assumed to be a rectangular area, $|v - u|$ is the Euclidean distance between the two points, u and v , and L is the correlation-scale parameter. Using the Cauchy-Gauss method [Journal and Huijbregts, 1978, p. 98], (A1) can be written as

$$I = \int_{-11}^{11} \int_{-12}^{12} \rho(|u|; L)(l_1 - |u_1|)(l_2 - |u_2|) du_1 du_2 \tag{A2}$$

$$I = 4 \int_0^{11} \int_0^{12} \rho(|u|; L)(l_1 - u_1)(l_2 - u_2) du_1 du_2 \tag{A3}$$

where u_1 and u_2 are the x and y coordinates of u and l_1 and l_2 are the sides of A along the x and y axes, respectively. The $\rho(|u|; L)$ value is assumed to be isotropic and Gaussian with no nugget effect [Journal and Huijbregts, 1978, p. 165]; i.e.,

$$\rho(|u|; L) = \exp \{-(u_1^2 + u_2^2)/L^2\} \tag{A4}$$

Then, from (A3), we have

$$I = l_1 l_2 L^2 \pi \operatorname{erf}(l_1/L) \operatorname{erf}(l_2/L) - l_1 L^3 \pi^{1/2} \operatorname{erf}(l_1/L) \{1 - \exp(-l_2^2/L^2)\} - l_2 L^3 \pi^{1/2} \operatorname{erf}(l_2/L) \{1 - \exp(-l_1^2/L^2)\} + L^4 \{1 - \exp(-l_1^2/L^2)\} \{1 - \exp(-l_2^2/L^2)\} \tag{A5}$$

where $\operatorname{erf}(\)$ denotes the error function.

Acknowledgment. This research was supported in part by NOAA (Climate and Global Change Research Program, grant NA36690419). This support is gratefully acknowledged.

References

- Anderson, E. A., National Weather Service River Forecasting System—Snow accumulation and ablation model, *NOAA Tech. Memo NWS HYDRO-17*, U.S. Dep. Comm., Silver Spring, Md., 1973.
- Barancourt, C., J. D. Creutin, and J. Rivoirard, A method for delineating and estimating rainfall fields, *Water Resour. Res.*, 28(4), 1133–1144, 1992.
- Eagleson, P. S., and Q. Wang, Moments of catchment storm area, *Water Resour. Res.*, 21(8), 1185–1194, 1985.
- Entekhabi, D., and P. S. Eagleson, Land surface hydrology parameterization for atmospheric general circulation models including sub-grid scale spatial variability, *J. Clim.*, 2, 816–831, 1989.
- Hudlow, M. D., Technological developments in real-time operational hydrologic forecasting in the United States, *J. Hydrol.*, 102, 69–92, 1988.
- Journel, A., and C. J. Huijbregts, *Mining Geostatistics*, Academic, San Diego, Calif., 1978.
- Klazura, G. E., and D. A. Imy, A description of the initial set of analysis products available from the NEXRAD WSR-88D system, *Bull. Am. Meteorol. Soc.*, 74(7), 1293–1311, 1993.
- Rodriguez-Iturbe, I., and J. M. Mejia, On the transformation of point rainfall to areal rainfall, *Water Resour. Res.*, 10(4), 729–735, 1974.
- Seo, D.-J., Nonlinear estimation of spatial distribution of rainfall—An indicator cokriging approach, *Stoch. Hydrol. Hydraul.*, in press, 1996.
- Seo, D.-J., and J. A. Smith, Rainfall estimation using rain gauges and radar—A Bayesian approach, 2. An application, *Stoch. Hydrol. Hydraul.*, 5, 31–44, 1991.
- Seo, D.-J., and J. A. Smith, On the relationship between catchment scale and climatological variability of surface-runoff volume, *Water Resour. Res.*, 32(3), 633–643, 1996.
- Seo, D.-J., R. A. Fulton, J. P. Breidenbach, D. E. Miller, and E. F. Friend, Final report for interagency memorandum of understanding among the NEXRAD program, WSR-88D Oper. Support Facil. and the Natl. Weather Serv. Off. of Hydrol., Hydrol. Res. Lab., Jan. 1995.
- Smith, J. A., and W. F. Krajewski, Estimation of parameters for the NEXRAD rainfall algorithms, Final report to hydrologic research laboratory, Off. of Hydrol., Natl. Weather Serv., Natl. Ocean. Atmos. Admin., Silver Spring, Md. 1994.
- Smith, J. A., D.-J. Seo, M. L. Baeck, and M. D. Hudlow, An inter-comparison study of NEXRAD precipitation estimates, *Water Resour. Res.*, in press, 1996.
- World Meteorological Organization and the International Council of Scientific Unions, The scientific plan for the GEWEX continental-scale international project, Rep. *WCRP-67 WMO/TD-416*, Geneva, Feb. 1992.

D.-J. Seo, Hydrologic Research Laboratory, W/073, National Weather Service, 1325 East-West Highway, Silver Spring, MD 20910. (e-mail: djseo@skipper.ssmc.noaa.gov)

J. A. Smith, Department of Civil Engineering and Operations Research, Princeton University, Princeton, NJ 08544.

(Received May 7, 1995; revised February 1, 1996; accepted February 9, 1996.)

